

Chapter 2

Femtosecond Laser Pulses

Since the birth of the laser, nearly 40 years ago, scientists have been continually interested in generation of ultrafast laser pulses in the picosecond and femtosecond time domain. The recent development of all-solid state femtosecond lasers, tunable in the visible and near-infrared spectral regions, has already shown an impact on spectroscopic investigations in different areas in physics, chemistry and biology. This chapter gives a brief introduction into the world of femtosecond laser pulses and the most frequently used techniques to measure such ultrashort pulses.

The operating principle of Ti:sapphire oscillators and Ti:sapphire amplifiers together with the generation of parametric effects is described in the first part of this chapter. The second part is devoted to the diagnostic techniques used in the present work which allow the measurement of these ultrafast events.

2.1 Generation of Femtosecond Laser Pulses

The central aim of this section is to give a concise introduction to nonlinear optics and to provide basic information about the most-widely used tunable femtosecond laser sources, in particular tunable Ti:sapphire oscillators and Ti:sapphire amplifiers or optical parametric amplifiers.

2.1.1 The Ti:sapphire Oscillator

In 1982, the first Ti:sapphire laser was built by Moulton [9]. The laser tunes from 680 nm to 1130 nm, which is the widest tuning range of any laser of its

class¹. Nowadays Ti:sapphire lasers usually deliver several Watts of average output power and produce pulses as short as 6.5 fs [11].

Time-Frequency Relationship

A pulse can be defined as a transient in a constant background. The shape of this pulse is the shape of this transient. Intuitively, the pulse shape can be represented by a bell-shaped function, such as a Gaussian function. It is known that the Fourier transform of a Gaussian function is also a Gaussian function. The general time and frequency Fourier transforms of a pulse can be written

$$E(t) = \frac{1}{2\pi} \int_{-\infty}^{+\infty} E(\omega) e^{-i\omega t} d\omega \quad (2.1)$$

and

$$E(\omega) = \int_{-\infty}^{+\infty} E(t) e^{i\omega t} dt \quad (2.2)$$

where $E(\omega)$ and $E(t)$ represent the frequency and time evolution of the electric field of the pulse, respectively. Since half-maximum quantities are experimentally easier to measure, the relationship between the duration and spectral bandwidth of the laser pulse can be written as [12]

$$\Delta\nu\Delta t \geq K \quad (2.3)$$

where $\Delta\nu$ is the frequency bandwidth measured at full-width at half-maximum (FWHM) with $\omega = 2\pi\nu$ and Δt is the FWHM in time of the pulse and K is a number which depends only on the pulse shape (see Table 2.1).

Thus in order to generate a laser pulse within femtosecond time domain one needs to use a broad spectral bandwidth. If the equality is reached in (2.3) one speaks about a Fourier-transform-limited pulse or simply a *transform-limited pulse*. One can also calculate the minimum time duration of a pulse giving a spectrum with $\Delta\lambda$ (nm) at FWHM, central wavelength λ_0 (nm) and the speed of light (m/s) c :

$$\Delta t \geq K \frac{\lambda_0^2}{\Delta\lambda \cdot c} \quad (2.4)$$

¹Other laser active media which provide laser pulses in the femtosecond time domain are Cr³⁺:LiSAF, Cr³⁺:LiCAF, Cr⁴⁺:YAG, Cr⁴⁺:Forsterite. More about in Ref. [10].

Function	$E(t)$	K
Gauss	$e^{-(t/t_0)^2/2}$	0.441
Hyperbolic secant	$1/\cosh(t/t_0)$	0.315
Lorentz	$1/[1 + (t/t_0)]^2$	0.142

Table 2.1: Different mathematical descriptions of a laser pulse and corresponding expression of the electric field. The constant K which determines the time-bandwidth product is given for each function as well.

Absorption transitions of sapphire crystals doped with Titanium (Ti^{3+}) ions occur over a broad range of wavelengths from 400 to 600 nm (see Figure 2.1). The emission band extends from wavelengths as short as 600 nm to wavelengths greater than 1 μm . This makes them suitable materials in constructing laser active media for generating femtosecond pulses. The long wavelength side of the absorption band overlaps with the short wavelength end of the emission spectrum. Therefore the laser action is only possible at wavelengths longer than 660 nm. Additionally, the tuning range is affected by mirror coatings, losses in the laser cavity, pump power, and pump mode quality [13]. The optics existing in the Ti:sapphire oscillators used in the present work (see also Chapter 4, sections 4.2.1 and 4.2.2) allow an unproblematic tunability between 750 nm and 850 nm, which corresponds to the wavelength range where the emission spectrum has a maximum.

Group Velocity Dispersion

The *Group Velocity Dispersion* (GVD) is defined as the propagation of different frequency components at different speeds through a dispersive medium. This is due to the wavelength-dependent index of refraction of the dispersive material. GVD causes variation in the temporal profile of the laser pulse, while the spectrum remains unaltered. A transform-limited pulse is also called short pulse or unchirped pulse. It is said that the initial short pulse will become *positively* chirped (or *upchirped*) after propagating through a medium with "normal" dispersion (e.g. silica glass). This corresponds to the situation when higher frequencies travel slower than lower frequencies (blue slower than red). The opposite situation, where the pulse travels through a medium with "anomalous" dispersion, leads to a *negative* chirp (or *downchirp*). Here the bluer frequencies propagate faster than the redder frequencies.

Sources of GVD are glass, prism sequences, diffraction gratings, etc.

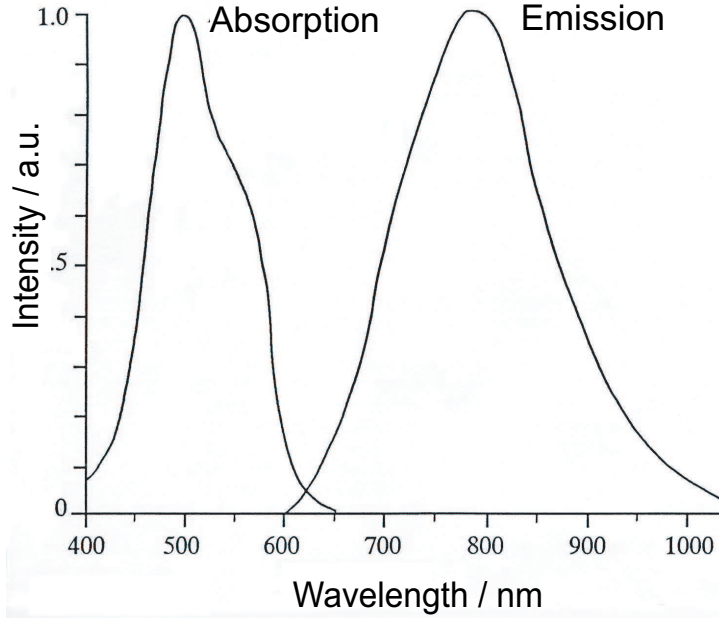


Figure 2.1: Absorption and emission spectra of the Ti:sapphire laser. The broad character of the absorption/emission spectra is due to the strong coupling between the vibrational energy states of the host sapphire crystal and the electronic energy states of the active Ti^{3+} ions [13].

The Kerr Lens Mode-locking

For simplicity, consider the spatial propagation of a Gaussian laser beam in a nonlinear material. The intensity profile of the beam is a function of its radius r and of a shape parameter g [12]. At high intensities, the refractive index depends nonlinearly on the propagating field. The lowest order of this dependence can be written as follows [12]:

$$n(r) = n_0 + \frac{1}{2}n_2I(r) \quad (2.5)$$

where n_2 is the nonlinear index coefficient and describes the strength of the coupling between the electric field and the refractive index n . According to Ref. [12] the intensity is:

$$I(r) = e^{-gr^2} \quad (2.6)$$

Hence, the refractive index changes with intensity along the optical path and it is larger in the center than at the side of the nonlinear crystal. This leads to the beam *self-focusing* phenomenon, which is known as the *Kerr lens effect* (see Figure 2.2). This process is enhanced along the optical path

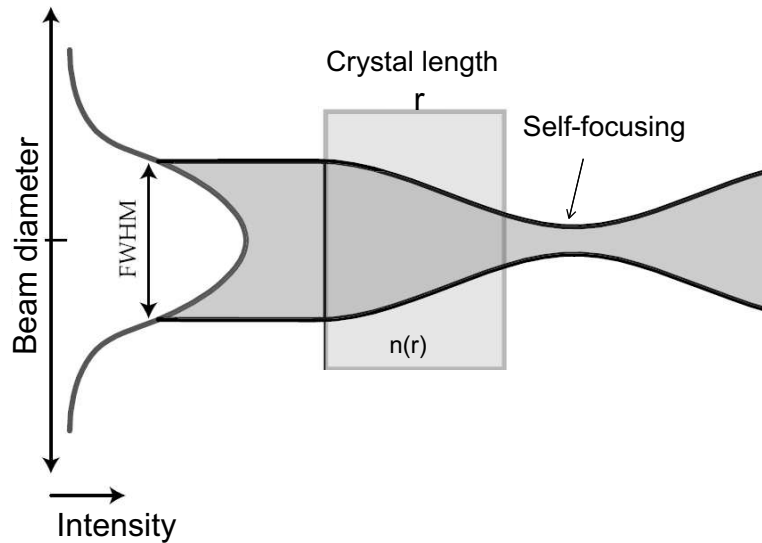


Figure 2.2: The Kerr lens effect and self-focusing. The index of refraction varies with intensity along the beam diameter. Depending on the sign of the nonlinear term n_2 in the expression (2.5) the index of refraction increases or decreases towards the center of the laser beam [12]. For positive n_2 the laser beam self-focuses.

because focusing the beam increases the focal "power" of this "lens". The increase of the focusing stops when the diameter of the beam is small enough and the linear diffraction is large enough to balance the Kerr effect.

Consider now a seed beam with a Gaussian profile propagating through a nonlinear medium, e.g. a Ti:sapphire crystal, which is pumped by a cw radiation. As aforementioned, for high intensity light, due to the intensity dependent refractive index, the Kerr lens effect occurs. When the laser operates in its most usual regime (*free-running laser*), it can oscillate simultaneously over all the resonance frequencies of the cavity. These frequencies make up the set of longitudinal modes of the laser. For the stronger focused frequencies, the Kerr lens favors a higher amplification. Thus the self-focusing of the seed beam can be used to suppress the cw operation, because the losses of the cw radiation are higher. Forcing all the modes to have equal phase (*mode-locking*) implies that all the waves of different frequencies will interfere (add) constructively at one point, resulting in a very intense, short light pulse [14]. The pulsed operation is then favored and it is said that the laser is mode-locked. Thus the mode-locking occurs due to the Kerr lens effect induced in the nonlinear medium by the beam itself and the phenomenon is known as *Kerr-lens mode-locking*.

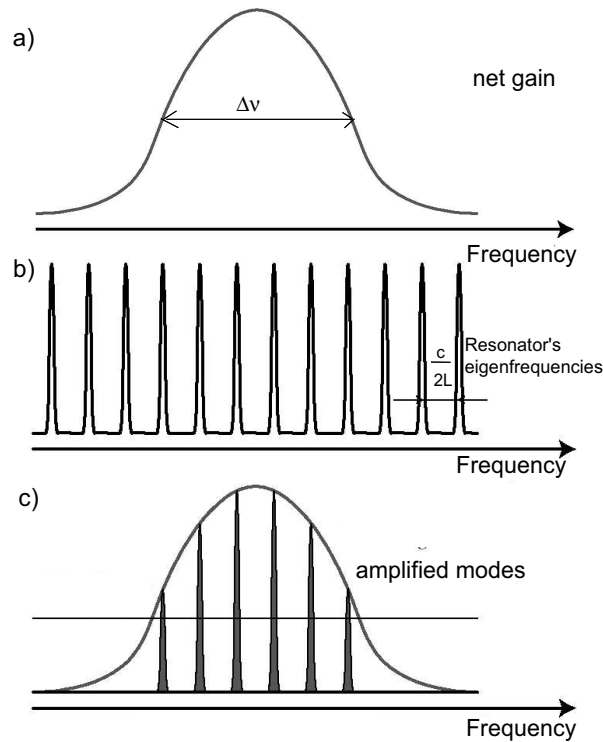


Figure 2.3: . The Kerr Lens Mode-Locking (KLM) principle. The axial modes of a laser cavity are separated by the intermode frequency spacing $\nu = c/2L$. (a) The net gain curve (gain minus losses). In this example, from all the longitudinal modes in the resonator (b), only six (c) are forced to have an equal phase [12].

The modes are separated in frequency by $\nu = c/2L$, L being the resonator length, which also gives the repetition rate of the mode-locked lasers:

$$\tau_{rep} = \frac{1}{T} = \frac{c}{2L} \quad (2.7)$$

Moreover the ratio of the resonator length to the pulse duration is a measure of the number of modes oscillating in phase. For example if $L = 1$ m and the emerging pulses have 100 fs time duration, there are 10^5 modes contributing to the pulse bandwidth.

There are two ways of mode-locking a femtosecond laser: *passive* mode-locking and *active* mode-locking.

Briefly, active mode-locking implies that the radiation in the laser cavity is modulated by a signal coming from an external clock source (e.g. acousto-optical modulator (AOM), electro-optical modulator). The modula-

tion frequency of the AOM is continuously adjusted to match the reciprocal cavity round trip time τ_{rep} by an algorithm which records the instantaneous repetition rate of the laser [15]. This method, also known as regenerative mode-locking, is used to initialize mode-locking in the Ti:sapphire oscillator (Spectra Physics Tsunami) described in Chapter 4, section 4.2.1, where the AOM works at 80 MHz.

The passive mode-locking technique does not require an external clock in the laser resonator. Here the laser radiation itself generates a modulation through the action of a nonlinear device (e.g. moving a prism into or out of the cavity) situated in the resonator. The modulation is automatically synchronized to the cavity round trip frequency. The Ti:sapphire oscillator (Kapteyn-Murnane) described in Chapter 4, section 4.2.2 uses the passive mode-locking technique.

One of the many advantages of Ti:sapphire oscillator is its high repetition rate (70–100 MHz). This allows a good duty cycle where the clusters in the molecular beam are irradiated several times by the output laser pulses of a relatively low energy (several nJ). Thus the laser operates in the weak-field regime. This avoids perturbation of potential energy surfaces (PES) produced by the intense laser pulse, simplifying the interpretation of the results (see also Chapters 8 and 9) and theoretical description. Moreover, non-resonant two-photon processes are not expected to occur.

2.1.2 The Ti:sapphire Amplifier

Several experiments require amplified laser pulses, e.g in Chapter 6. The output intensities are much higher than in a Ti:sapphire oscillator and could influence the dynamics of a molecule in the excited state, by perturbing the PES. The amplification of femtosecond laser pulses takes place also in a Ti:sapphire crystal, which is called *gain medium*², pumped by an external laser source (pump laser). A femtosecond Ti:sapphire oscillator serves as *seed* laser for the amplification process. In order to avoid the damage of the gain medium by the high intensities of the seed pulses, one needs to lower their peak power. This is achieved in the stretching step. The pulses can be then safely amplified. Later on they are recompressed to the initial duration. These concepts are briefly outlined in the following sections.

²Other materials used in femtosecond amplifiers are: alexandrite (Cr:Be₂O₃) 700–820 nm, Nd:glass 1040–1070 nm, colquirites(Cr:LiSAF, Cr:LICAF) 800–1000 nm, etc.

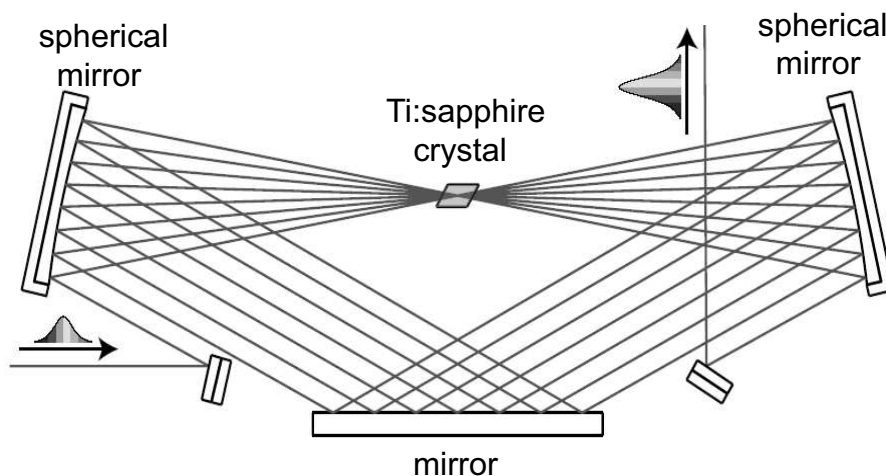


Figure 2.4: Schematic principle of a multipass amplifier.

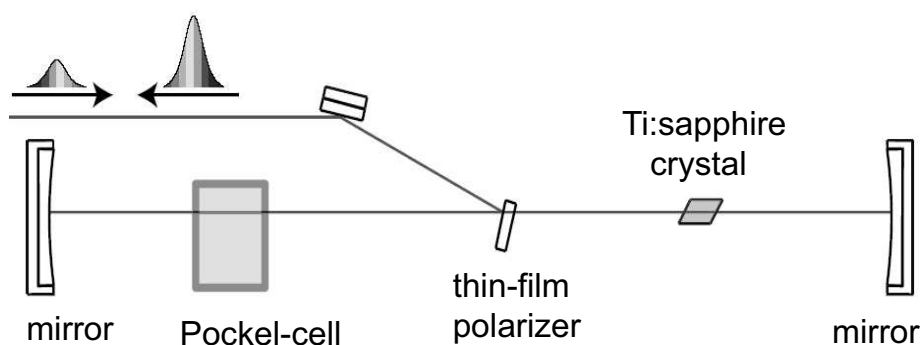


Figure 2.5: Schematic principle of a regenerative amplifier.

Multipass and Regenerative Amplification

Two of the most widely used techniques for amplification of femtosecond laser pulses are the multipass and the regenerative amplification.

In the *multipass amplification* different passes are geometrically separated (see Figure 2.4). The number of passes (four to eight) are usually limited by the difficulties on focussing all the passes on a single spot of the crystal. In the multipass amplifier existing in our laboratory (see section 4.2.2) there are eight passes. The amplifier bandwidth has to be broad enough to support the pulse spectrum. This is why Ti:sapphire crystals are widely used in the amplification process.

The *regenerative amplification* technique implies trapping of the pulse to be amplified in a laser cavity (see Figure 2.5). Here the number of passes is

Stretcher-Compressor

By using a dispersive line (combination of gratings and/or lenses), the individual frequencies within a femtosecond pulse can be separated (stretched) from each other in time (see Figure 2.6a). The technique, called *chirped pulse amplification* (CPA), has been introduced by Mourou [16]. The duration of the incoming femtosecond pulse is stretched (chirped) up to 10^4 times in order to reduce the pulse peak intensity. The pulse is now ready to be amplified, since its amplification gain is lower than the damage threshold of the amplification crystal. After amplification the pulse is recompressed to its original duration by a conjugate dispersion line (with opposite GVD). The recompression stage takes place in the compressor (see Figure 2.6b).

The main problem the compressor has to deal with is that it has to recover not only the initial pulse duration and quality, but it has to compensate the dispersion introduced in the amplification stage itself. To overcome this problem, the distance between gratings in the compressor has to be larger than in the stretcher. This will cancel overall second-order dispersion and help in producing relatively short pulses, but also introduces higher-order dispersion terms, which will reflect in prepulses and/or wings.

2.1.3 Parametric Effects

The experiments presented in Chapter 7 were performed with the two parametric amplifiers within the femtosecond laser system described in Chapter 4, section 4.2.2. The reason is that the excitation wavelength required for the first electronic excited state of the Na_2F molecule is outside the wavelength range (750–850 nm) of the Ti:sapphire oscillators/amplifiers. This section gives a brief introduction of the parametric effects used to generate other frequencies.

In nonlinear optics the Taylor expansion of the macroscopic polarization \mathbf{P} of a medium when it is illuminated by the electric field \mathbf{E} is [12]

$$\mathbf{P} = \chi^{(1)}\mathbf{E} + \chi^{(2)}\mathbf{E}\mathbf{E} + \chi^{(3)}\mathbf{E}\mathbf{E}\mathbf{E} \quad (2.8)$$

where the linear first-order term in the electric field describes linear optics, refractive index, absorption, the quadratic second-order term accounts for nonlinear optical effects, second-harmonic generation, parametric interactions and the cubic third-order term describes processes like third-harmonic generation.

The second-order susceptibility $\chi^{(2)}$ is responsible for a variety of nonlinear optical effects, in which one photon is split into two other photons

or two photons can mix to generate a third one. Maybe the most important phenomena are the second-harmonic generation (SHG) and parametric effects.

Briefly, in SHG a pair of photons with the same frequency ω , can mix together in a nonlinear material³ with high second-order susceptibility and give rise to a single photon with twice the original frequency. Hence, the energy of the outgoing photons is twice the energy of the incoming one. The frequency conversion is valid only when the energy and momentum are conserved. The intensity $I(2\omega)$ of the second harmonic varies with the square of the incident intensity $I^2(\omega)$.

There are two types of frequency-doubling crystals: type I, when the two mixing photons have the same polarization and type II, when the two mixing photons are orthogonally polarized. The doubling crystals have to match the full width of the incoming spectrum.

The *parametric effects* involve three photons and generation of new frequencies. In a nonlinear quadratic crystal, a single photon having the frequency ω_3 produces two photons: one with the frequency of ω_1 (*signal*) and another one with the frequency of ω_2 (*idler*):

$$\omega_1 + \omega_2 = \omega_3 \quad (2.9)$$

where $\omega_1 > \omega_2$. This phenomenon is called *optical parametric generation* (OPG). An optical parameter amplifier is then a laser where the optical radiation is produced in a parametric crystal and not by inversion of population. Similarly, an optical parameter oscillator (OPO) operates on the basis of the same phenomenon, but the parametric crystal is situated in a resonator.

In a *parametric up-conversion* or *sum frequency generation*, two pulses having the frequencies of ω_1 and ω_2 are sent through a birefringent crystal and generate a pulse of frequency

$$\omega_3 = \omega_1 + \omega_2 \quad (2.10)$$

Furthermore, in *parametric down-conversion* or *frequency difference* two photons of frequencies ω_1 and ω_2 are sent in a nonlinear medium and they generate a photon having the frequency difference of the two incident photons

$$\omega_3 = \omega_2 - \omega_1 \quad (2.11)$$

These three-wave mixing processes occur only if the energy and momentum are conserved:

³The birefringent crystals, such as LBO (lithium triborate), BBO (β -barium borate), KTP (KTiOPO₄), etc., have a large $\chi^{(2)}$.

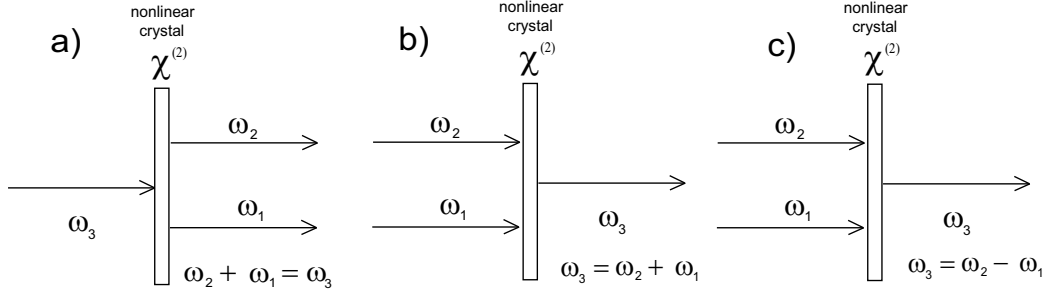


Figure 2.7: Parametric interactions: a) optical parametric generation; b) parametric up-conversion (sum-frequency); c) parametric down-conversion (frequency-difference). The use of one of these nonlinear optical processes of second order leads to the generation of new frequencies.

$$\hbar\omega_3 = \hbar\omega_1 + \hbar\omega_2 \quad (2.12)$$

and

$$\vec{k}_3 = \vec{k}_1 + \vec{k}_2 \quad (2.13)$$

Here the \vec{k}_j represent the wave vectors of each of the three waves. If the three waves propagate collinearly, the expression (2.13), also known as *phase-matching condition* can be written

$$\frac{n_3}{\lambda_3} = \frac{n_1}{\lambda_1} + \frac{n_2}{\lambda_2} \quad (2.14)$$

Thus one has to use birefringent crystals, where the waves can propagate with different polarizations. This is because in normal materials, where the refractive index varies as $1/\lambda$, this condition can never be fulfilled. The parametric interaction can be tuned by modifying the angle between the optical axis of the nonlinear crystal and the direction of propagation. The wavelength changes as long as the phase-matching condition is satisfied. Certainly this should be valid over the whole spectrum of the input pulse. In practice, this implies the use of only thin crystals, because in a first approximation, the parametric interaction efficiency is proportional to the product of the intensity and the interaction length. Thereby, the GVD, which tends to chirp the short pulses and to reduce their peak power, will be compensated for each wavelength, too. Due to these characteristics, parametric oscillators and amplifiers have a very broad tunable range (hundreds even thousands of nanometers).

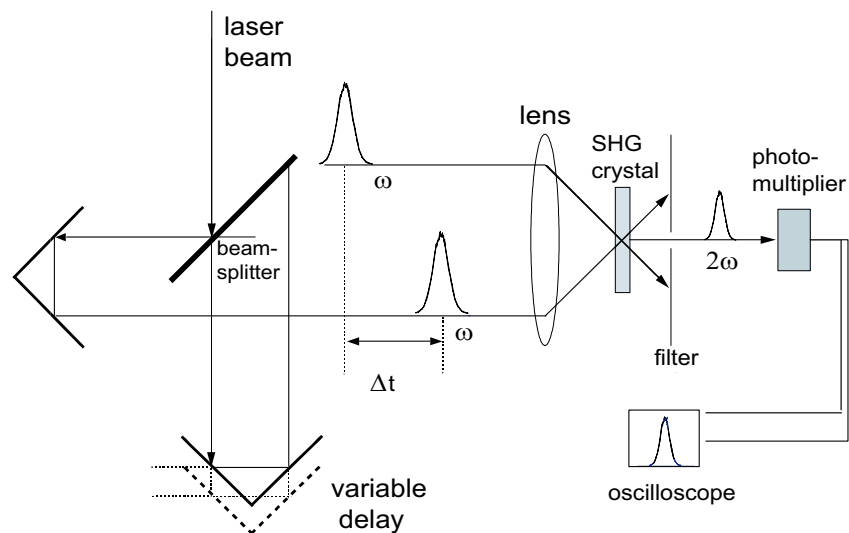


Figure 2.8: Schematic principle of non-collinear SHG auto-correlation: the input pulse is split into two; the two pulses are recombined and focused onto the nonlinear medium; the SHG auto-correlation is detected by a photo-multiplier, whereas the fundamental input light is blocked by a filter.

2.2 Diagnostic Techniques

Before femtosecond laser pulses are used in experiments pulse diagnostics are necessary. Since the femtosecond time scale is beyond the range of the fastest electronics, the pulse measurement techniques have to be redesigned in order to fully characterize the amplitude and the phase of the electric field. This section will briefly describe the standard techniques in determining the temporal profile of the pulse, such as auto-correlation and cross-correlation. Other techniques, which are more sophisticated give information about both frequency and time, such as F.R.O.G. and XFROG/STRUT. All these techniques have been used in the present work.

2.2.1 Auto-correlation

Maybe the most widely used technique for measuring femtosecond laser pulses is the second-order auto-correlation function, which was first demonstrated in 1966 by Maier and co-workers [17]. This method takes advantage of the second harmonic generation in nonlinear crystals. In Figure 2.8 the basic principle of SHG auto-correlation is displayed. This is typically used to measure the time duration of femtosecond pulses.

Pulse shape	I(t)	Time-bandwidth Product $\Delta\nu \cdot \Delta t$	$\frac{\Delta\tau}{\Delta t}$
Gaussian	$\exp\left(-\frac{4\ln 2 t^2}{\Delta t^2}\right)$	0.441	$\sqrt{2}$
Secant hyperbolic	$\operatorname{sech}^2\left(\frac{1.76t}{\Delta t}\right)$	0.315	1.55
Lorentz	$1/\left(1 + \frac{2t}{\Delta t}\right)^2$	0.221	2

Table 2.2: Examples of pulse shapes, their time-bandwidth products and the conversion factors for determining the pulse duration (at FWHM).

The incident laser pulse is split in two pulses by a 50/50 beam-splitter. Similar to a Michelson interferometer, the two pulses are reflected in each arm and subsequently focused onto a frequency-doubling crystal. The resulting SHG auto-correlation trace is detected by a photo-multiplier as a function of the time delay Δt between the two pulses. The SHG crystals can be type I phase-matching or type II, and the two pulses can recombine collinearly or non-collinearly in the frequency doubling medium.

If the two fields are of intensity $I(t-\tau)$ and $I(t)$, the auto-correlation of the two pulses is

$$A_{ac}(\tau) = \int_{-\infty}^{\infty} I(t)I(t-\tau)dt \quad (2.15)$$

The auto-correlation is always a symmetric function in time. Unfortunately, it gives very little information about the shape of the pulse, since an infinity of symmetric and asymmetric pulse shapes can have similar auto-correlation. The most widely used procedure to determine the pulse duration is to "assume" a pulse shape (usually sech^2 or a Gaussian shape, for chirp-free and linear chirped pulses) and to calculate the pulse duration from the known ratio between the FWHM of the auto-correlation and of the pulse. Thus the auto-correlation function depends on the assumed shape of the pulse. Table 2.2 lists the relevant parameters for various shapes.

More information about the auto-correlation and the employed auto-correlator can be found in Refs [12, 14, 18, 19].

2.2.2 Cross-correlation

The major difference between the auto-correlation technique and the cross-correlation is that in the latter the femtosecond pulse is not correlated with itself (the two (sub)pulses are not identical).

The cross-correlation implies the use of a reference pulse of a known shape $I_r(t)$ in order to determine the temporal profile of an unknown laser pulse, $I_s(t)$. The intensity cross-correlation to be measured can be written as

$$A_{cc}(\tau) = \int_{-\infty}^{\infty} I_s(t)I_r(t - \tau)dt \quad (2.16)$$

The convolution with the intensity of the reference pulse leads to a smoothing of the pulse shape. If the pulse to be measured consists of a few subpulses, the time separation between the subpulses in the cross-correlation trace remains unchanged [20]. The cross-correlation of pulses with longer time duration than the reference pulses corresponds in a first approximation to the actual temporal profile of the pulse. The intensity cross-correlation does not provide any information about the phase of the pulse. The phase of the laser pulse to be measured can be extracted from the FROG and/or XFROG/STRUT traces, respectively (see sections 2.2.3 and 2.2.4).

The setup for recording cross-correlation traces is similar to the setup presented in Figure 2.8 with the difference that one pulse has different characteristics (central wavelength and/or pulse shape).

2.2.3 F.R.O.G.

The usual methods for measuring femtosecond pulses, such as cross-correlation or the SHG autocorrelation do not provide phase information nor do they enable the correct determination of the intensity. If one wants to measure a complicated pulse shape, these techniques provide only limited information.

Measurements in the time-frequency domain involve both temporal and frequency resolution simultaneously. A well-known example of such a measurement is illustrated by a musical phrase, where the frequencies present in an acoustic waveform are shown during a time interval. Thus a sonogram, like depicted in Figure 2.9, is a plot of the waveform's frequency versus time, with additional information indicating the intensity (e.g. pianissimo or fortissimo).

The F.R.O.G. (*Frequency-Resolved Optical Gating*) technique [21] is based on the above mentioned similarities with the musical phrase and is a newly developed method to measure the characteristics of a laser pulse in both time and frequency domains. FROG is basically a spectrally resolved auto-correlation measurement. The pulse to be measured is split into two identical pulses, which are recombined in a nonlinear crystal, as in auto-correlation. The signal pulse is later spectrally resolved by a grating and imaged by a CCD array. The two-dimensional image is called FROG trace. The FROG technique is not limited to amplified pulses (mJ). Pulses of μJ even nJ energy can be measured.

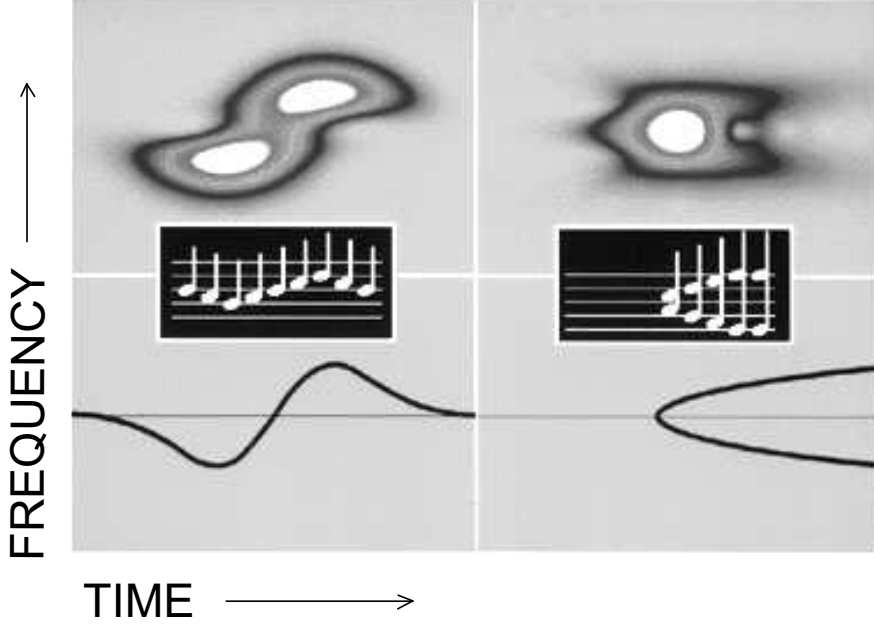


Figure 2.9: The spectrogram and the sonogram follow the pulse frequency vs. time (left) or the group delay vs. frequency (right).

The spectrogram

$$S(\omega, \tau) = \left| \int_{-\infty}^{\infty} E(t)g(t - \tau)e^{-i\omega t} dt \right|^2 \quad (2.17)$$

is sufficient to completely characterize the electric field $E(t)$. Here $g(t - \tau)$ is the variable-delay gate function. In the case of the SHG FROG⁴, used in this work to characterize the laser fields, $g(t - \tau) = E(t - \tau)$ i.e. the pulse is measured with itself by splitting it into two identical subpulses. The expression (2.17) becomes [21]:

$$I_{FROG}^{SHG}(\omega, \tau) = \left| \int_{-\infty}^{\infty} E(t)E(t - \tau)e^{-i\omega t} dt \right|^2 \quad (2.18)$$

⁴Besides SHG FROG, there are other beam geometries used to measure ultrashort pulses, such as polarization gate (PG FROG), third harmonic generation (THG FROG), transient grating (TG FROG), self-diffraction (SD-FROG), TADPOLE (combination of FROG and spectral interferometry) or the recent GRENOUILLE. More about the different FROG techniques can be found in [19, 21].

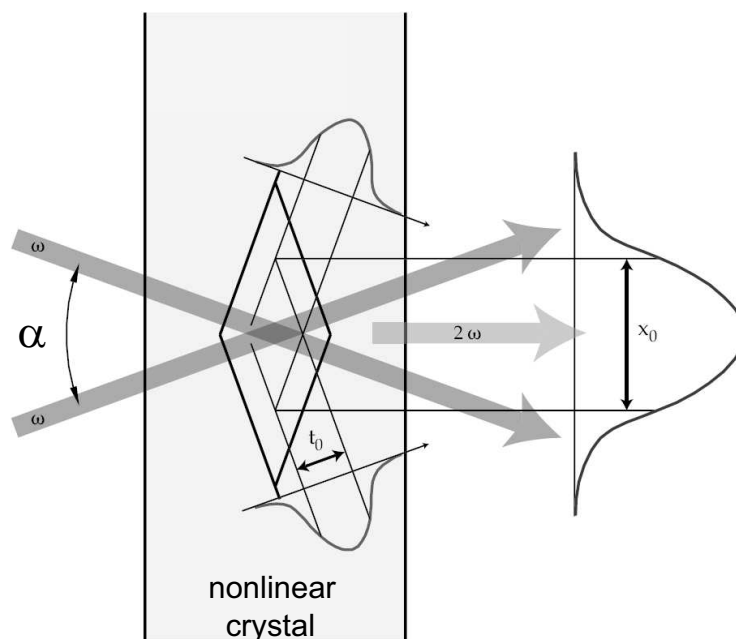


Figure 2.10: Principle of a single-shot autocorrelator. The pulse to be measured is split in two equal replicas at frequency ω , which are collimated by a cylindrical lens in a nonlinear crystal. The beams intersect at angle α . The SHG signal 2ω contains temporal information about the pulse. Thus the delay varies along the nonlinear crystal on the x -axis. A grating splits the SHG light into its frequency components and a CCD array allows to resolve both the temporal and spectral distribution of the femtosecond pulse and measures them in a single shot.

Single-Shot SHG FROG

The SHG FROG used in this work is based on single-shot measurements, meaning that every single pulse is measured. The SHG signal is created in a single-shot auto-correlator [22]. The incoming pulse is split in two by a beam-splitter and focused by a cylindrical lens in a BBO crystal, oriented for type I SHG. The angle between the two pulses is around $\alpha = 25^\circ$ and is responsible for the resolution and the maximum recordable pulse duration [23]. Then the intensity distribution of the SHG signal is measured by a two-dimensional detector (CCD camera⁵). The recordable two-dimensional image displays on-line the time and the wavelength axes.

In Figure 2.10 the principle of a single-shot auto-correlator is shown. The crossed wavefronts induce a second-order process and transform the temporal

⁵Kappa ImageBase, model CF 8/1 DX II, Gleichen, Germany.

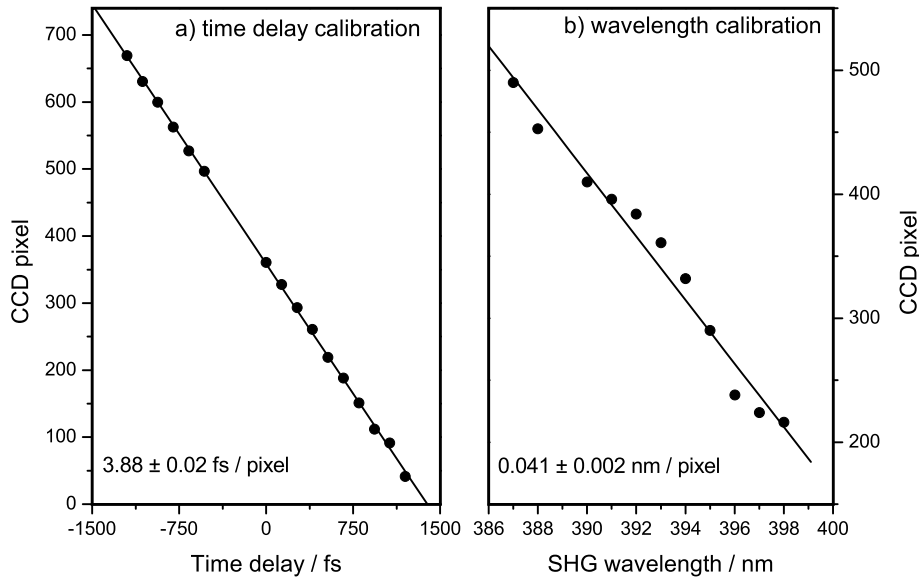


Figure 2.11: Calibration curves recorded for the CCD window in the SHG FROG apparatus: (a) Time delay calibration. The dots represent the central pixel position of the FROG traces at every delay time in-between. The line represents the linear fit and gives the result of 3.88 fs/pixel. Extrapolating the linear function, the time window of the CCD array corresponds to 2.87 ps; (b) Wavelength calibration. This was recorded by changing the central wavelength of the laser and reading the SHG signal for central pixel of each FROG trace. One pixel corresponds to 0.041 nm, whereafter the entire wavelength window of the CCD camera totals 23.7 nm.

distribution of the pulse into a spatial intensity distribution of the SHG signal generated in the nonlinear crystal along the x -axis. The geometric analysis allows the calculation of the initial pulse duration from the spatial distribution of the SHG pulse.

The time and wavelength axes of the CCD window (740×580 pixels) have to be calibrated. For the time calibration, one needs to record a few FROG traces at different time delays. This is done inside the FROG apparatus by changing the position of the micrometer screw on which a retroreflector is mounted. The position of the central pixel for every FROG trace is recorded. The distance between the central pixels of each spectrogram corresponds to the time delay between the FROG spectrograms. The curve is then extrapolated for the entire window. For the calibration of the wavelength axis, one needs to tune the laser frequency and monitor the position of the central pixel in the FROG trace on the CCD array. The results of the calibration procedure

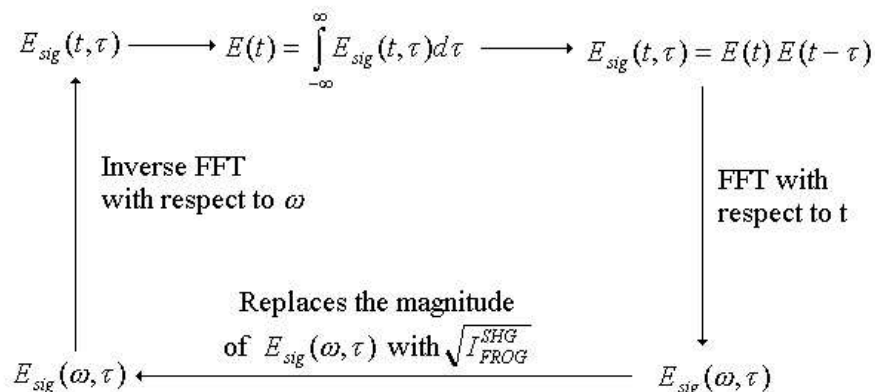


Figure 2.12: Iterative Fourier-transform algorithm for inverting a FROG trace to obtain the intensity and phase of an ultrashort pulse.

are shown in Figure 2.11: for the time calibration there are 3.88 fs/pixel and 0.041 nm/pixel for the wavelength axis, corresponding to a time window of 2.871 ps and to a wavelength window of 23.7 nm, respectively. For a detailed calibration measurement, see Ref. [19].

The SHG FROG trace is always symmetric with respect to the time axis, which leads to an ambiguity in the retrieved electric field in time. For this reason, SHG FROG trace cannot distinguish between a pulse and its time-reverse replica and is identical for a pulse with positive or negative chirp. Information about the time evolution of the phase and amplitude of the electric field can be obtained from the phase-retrieval algorithm (see the following section).

Phase-retrieval Algorithm

The FROG uses a phase-retrieval algorithm to retrieve the intensity and the phase from a measured spectrogram of an ultrashort laser pulse. This is because spectrogram inversion algorithms require knowledge of the gate function [21]. The algorithmic method which gives the most robust solutions and was used also in this work is called *generalized projections* [24]. Genetic algorithms [25] or other algorithms [26] can be employed. The goal of the phase-retrieval algorithm is to find the $E(t)$ or equivalently $E_{sig}(t, \tau)$, which satisfies two constraints: (i) the data constraint

$$I_{FROG}(\omega, \tau) = \left| \int_{-\infty}^{\infty} E_{sig}(t, \tau) e^{-i\omega t} dt \right|^2 \quad (2.19)$$

and (ii) the nonlinear optical constraint, particular for each beam geometry used in the measurement. For SHG FROG the nonlinear optical constraint can be written as

$$E_{sig}(t, \tau) \propto E(t)E(t - \tau). \quad (2.20)$$

From an initial guess of the electric field $E_{sig}(t, \tau)$, a spectrogram is calculated and compared to the measured spectrogram. The deviation is iteratively minimized until the algorithm converges. The amplitude and the phase are extracted from the retrieved (reconstructed) electric field. The root-mean-square difference between the measured and the computed trace from the retrieved pulse field is called the FROG error. The program used for retrieving the electric field of the laser pulse measured with SHG FROG technique is described in Appendix B.

2.2.4 XFROG/STRUT

Due to the limited time window of the CCD array in the SHG FROG apparatus, pulses with a duration higher than 2.8 ps cannot be measured. Moreover, the SHG FROG is not recommended for very complicated pulses, since it gives a non-intuitive information about the laser pulse due the temporal ambiguity (one needs to use the phase-retrieval procedure). The laser pulses obtained in the experiments described in the Chapters 8 and 9 were measured by employing a *multi-shot* technique: XFROG (cross-correlation FROG). This technique is also known as STRUT (Spectrally and Temporally Resolved Up-conversion Technique) [27–29]. The advantage of this method is that the spectrogram has an intuitive form and one can distinguish the temporal behavior of the frequencies within the laser pulse. Moreover, the electric field can be reconstructed for very complicated pulses.

The intensity cross-correlation signal (*sum-frequency generation*), described in section 2.2.2, is generated in a nonlinear crystal (BBO, type I, SFG) and subsequently spectrally resolved by a spectrometer (see Figure 2.13). The wavelength range is split into a few wavelength intervals $\Delta\lambda$ (typically 40 or 60). For every wavelength interval $\Delta\lambda$ a cross-correlation trace is recorded. By adding all cross-correlation traces for each wavelength interval, one obtains the XFROG trace. The technique is multi-shot because of the scanning procedure. The XFROG spectrogram contains a two-dimensional image, whereby one axis represents the wavelength and the other axis is the time. The resolution of the spectrometer⁶ used is $\Delta\lambda = 0.02$ nm and allows measurements in a large spectral domain (190 nm–40 μm). The optical

⁶Jobin Yvon GmbH, model HR 250 S, München, Germany.

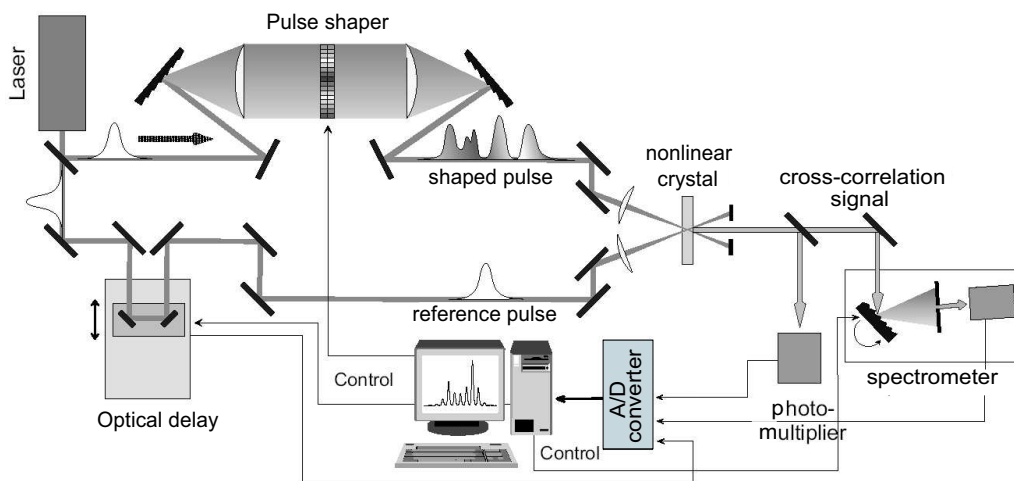


Figure 2.13: Schematic principle of temporal and wavelength-resolved cross-correlation: the input pulse is split into two; the shaped pulse to be measured is recombined with the reference pulse and focused onto the nonlinear crystal; the SFG cross-correlation trace is detected by a photo-multiplier as a function of time delay between the two pulses. By sending the cross-correlation signal into a spectrometer and recording cross-correlation traces at different wavelengths, one can obtain information about both wavelength and time duration of the shaped pulse (XFROG/STRUT traces).

delay stage provides a time resolution for the scan of $\Delta t < 0.5$ fs. In this work the XFROG traces were recorded with a spectral resolution of typically $\Delta\lambda = 0.2\text{--}0.4$ nm and a time resolution of the cross-correlation scan of $\Delta t = 10\text{--}40$ fs.

The up-converted optical signal at the SHG crystal has the following form [30]:

$$E_{up}(\omega, \tau) \propto \int_{-\infty}^{+\infty} E_r(\omega') \exp(i\omega'\tau) E_t(\omega - \omega') d\omega'. \quad (2.21)$$

Here τ represents the optical time delay between the pulses in the cross-correlation arms (the test pulse towards the reference pulse) and ω is the detuning from the central frequency (the up-converted frequency).

The XFROG trace is proportional to the squared magnitude of the spectrum of the cross-correlation signal [31]:

$$I_{XFROG}(\Omega, \tau) \propto \left| \int_{-\infty}^{+\infty} E_{up}^{FT}(t, \tau) \exp(i\Omega t) dt \right|^2, \quad (2.22)$$

where $E_{up}^{FT}(t, \tau)$ is the Fourier transform of the expression (2.21) and Ω is the central frequency.

For a quantitative evaluation of the phase and the amplitude of the electric field, a phase-retrieval algorithm is required for reconstructing the electric field from the XFROG trace. The numerical algorithm is based on the generalized projections method. The corresponding software is contained in the FROG 3.0 package⁷. Details about the XFROG method can be found in Ref. [31].

For measuring the pulse shapes presented in Chapter 9, a setup for recording both temporal and spectral cross-correlation traces of shaped femtosecond pulses with unshaped pulses has been constructed (see Figure 2.13). By using a computer program, one can rapidly measure background-free intensity cross-correlations with a resolution of a few femtoseconds. The signal recorded is not a SHG signal but a SFG (sum-frequency generation in the UV domain) signal generated in the nonlinear BBO crystal. By employing a high-resolution spectrometer one can also record XFROG/STRUT traces, which provides information about both wavelength and temporal profile of the shaped laser pulse. After a phase-retrieval analysis, the amplitude and the phase of the electric field can be obtained from the XFROG/STRUT traces.

⁷Femtosoftware Technologies, Oakland, CA, U.S.A.